Revealing the Cooper minimum of N_2 by Molecular Frame High-Harmonic Spectroscopy

J. B. Bertrand,[1] H. J. Wörner,[2] P. Hockett,[1] D. M. Villeneuve,[1] and P. B. Corkum[1]

[1]*Joint Attosecond Science Laboratory, National Research Council of Canada and University of Ottawa, 100 Sussex Drive, Ottawa, K1A 0R6, Canada*

[2]*Laboratorium für physikalische Chemie, ETH Zürich, Wolfgang-Pauli-Strasse 10, 8093 Zürich, Switzerland*

(Received 26 March 2012; published 4 October 2012)

Molecular frame high-harmonic spectra of aligned N_2 molecules reveal a Cooper-like minimum. By deconvolving the laboratory frame alignment distribution, what was previously thought to be a maximum of emission along the molecular axis is found to be maxima at 35 degrees off axis, with a spectral minimum on axis. Both of these features are supported by photoionization calculations that underline the relationship between high-harmonic spectroscopy and photoionization measurements. The calculations reveal that the on axis spectral minimum is a Cooper-like minimum that arises from the destructive interference of the p and f partial wave contributions to high-harmonic photorecombination. Features such as Cooper minima and shape resonances are ubiquitous in molecular photoionization or recombination.

DOI: 10.1103/PhysRevLett.109.143001 PACS numbers: 33.20.−t, 82.53.Kp

The photoionization transition moment is an observable that contains important information about the electronic structure of molecules [1]. When measured in the molecular frame and over a wide spectral range, the transition moment allows us to image valence electronic structure [2–4] and to follow electronic [5] or chemical dynamics [6,7]. For decades, the photoionization transition moment could be measured using extreme ultraviolet (XUV) radiation produced by a synchrotron [8]. However, retrieving the molecular frame XUV photoionization signal from valence molecular orbitals is challenging because the long pulse duration of the ionizing radiation ($\sim$ 100 ps) [9] prevents the use of field-free molecular alignment techniques ($\sim$ 100 fs) [10].

An alternative approach, high-harmonic spectroscopy, can measure the photorecombination transition moment over a wide range of photon energies simultaneously [11–13]. The short duration of the high-harmonic process (a few tens of fs) allows the use of field-free molecular alignment. In high-harmonic spectroscopy, an intense femtosecond laser pulse removes a valence electron from the molecule. The laser field subsequently drives the electron back to the parent ion where it can radiatively recombine, resulting in the emission of an XUV photon in a phase matched process [14,15]. The recombination process is essentially the time reversal of photoionization, and can be treated as a measure of the same transition matrix elements [11,12].

Here we measure the high-harmonic spectrum of molecular nitrogen (N_2) in the photon range of 20–80 eV. We apply recently developed deconvolution methods to access the molecular frame response [16,17], revealing previously unseen features. We show that there is a minimum in the transition moment along the molecular axis at about 45 eV. We relate this to a Cooper-like minimum in which the transition moment goes through a minimum due to destructive interference between dominant partial wave components. The deconvolution shows that there are maxima at around 35 degrees off axis, which have not previously been observed in laboratory frame measurements. The measured transition moments are in good agreement with photoionization calculations. By performing the experiment at two different laser wavelengths (800 and 1200 nm), we verify that we measure the electronic structure and not dynamic interference between orbitals [18].

For the experiment, we impulsively align N_2 molecules [10] with a stretched, nonionizing pump pulse (70 ± 5 fs, 800 nm, $I_{\text{align}} = 5 \times 10^{13}$ W/cm^2) and probe the aligned molecules with an intense ionizing pulse (800 nm: 32 ± 2 fs or 1200 nm: 40 ± 5 fs, both with peak intensity $I_{\text{probe}} = 1.5 \times 10^{14}$ W/cm^2 determined from the high-harmonic cutoffs). The 800 nm pulses are generated by a Ti: Sapphire multipass laser system (32 fs, 800 nm, 50 Hz, 12 mJ per pulse) and the 1200 nm pulses ($\sim$ 1 mJ) are generated by a high-energy optical parametric amplifier (HE-TOPAS) pumped with 800 nm light. The high-harmonic experimental chamber consists of a source chamber, a pulsed valve (250 μm orifice), an XUV grating, a microchannel plate detector backed by a phosphor screen, and a camera readout.

High-harmonic spectra are recorded at maximal alignment, around the first rotational half-revival (4.12 ps). In the laboratory frame, we vary the angle α between the alignment distribution axis and the probing field by rotating the alignment (pump) beam polarization (both beams are linearly polarized). In Fig. 1, we show laboratory frame high-harmonic spectra taken with (a) 800 and (b) 1200 nm light. For both wavelengths, the experimentally observed high-harmonic yields peak along $\alpha = 0°$, as also previously reported at 1300 nm in Ref. [19]. A spectral minimum is located in the vicinity of $\sim$42 eV and $\alpha = 0°$. The

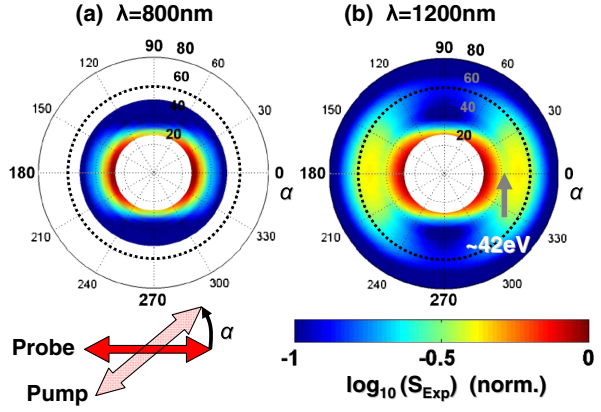

FIG. 1 (color online). Experimentally recorded high-harmonic signal from aligned N_2 as a function of alignment angle α for two probe-pulse central wavelengths (800 or 1200 nm) at $I_{\text{probe}} = 1.5 \times 10^{14}$ W/cm^2. The radius of the polar plots corresponds to photon energies in the range of 0–80 eV, while the angle corresponds to the angle α between the probe polarization and the molecular alignment. The black dotted line marks 60 eV. The color scale is logarithmic.

minimum is evident with a 1200 nm laser wavelength, but is not seen with 800 nm in the present experiment due to a lower cutoff. The minimum was previously observed around 40 eV at 800 nm but with higher laser intensity [2,20].

The high-harmonic signal measured in the laboratory frame, $S(\Omega, \alpha)$, is a coherent convolution of the molecular frame dipole field $\vec{D}(\Omega, \theta)$ with the prolate alignment distribution $A(\theta', \phi')$, where θ is the angle between the laser field polarization and the molecule's internuclear axis, θ' and ϕ' are the zenithal and azimuthal angle with respect to the alignment distribution axis, and Ω is the harmonic frequency. The angle θ is given by the laboratory to molecular frame coordinate transformation: $\cos\theta = \cos\alpha \cos\theta' - \sin\alpha \sin\theta' \sin\phi'$ [16]. In the molecular frame, the emitted high-harmonic complex dipole field $\vec{D}(\Omega, \theta)$ can be considered in the 3-step model and therefore contains contributions from ionization, propagation, and recombination processes [14]. To extract the molecular frame high-harmonic dipole from amplitude (XUV signal)-only measurements, we make the approximation that the dipole phase varies slowly ($\ll \pi$) within the alignment distribution ($\sim 25°$ FWHM). It allows us to add the contribution from all angles incoherently as done previously [17]. This assumption will likely fail in the occurrence of a rapid variation of the angular phase caused, for example, by the presence of nodal planes in the highest occupied molecular orbital (HOMO) and/or the interplay of multiple orbitals [5].

In the experiment, we do not distinguish parallel and perpendicular polarization components, with respect to the driving laser (linear) polarization axis, of $\vec{D}(\Omega, \theta)$. Therefore, we group them directly as the total molecular frame dipole amplitude $|\vec{D}(\Omega, \theta)| = \sqrt{|D_{\parallel}(\Omega, \theta)|^2 + |D_{\perp}(\Omega, \theta)|^2}$. Based on this approach, the integral form for the measured laboratory frame high-harmonic signal $S(\Omega, \alpha)$ becomes [21]

$$\sqrt{S(\Omega, \alpha)} \approx \int_{\theta'=0}^{\theta'=\pi} \int_{\phi'=0}^{\phi'=2\pi} \Omega^2 |\vec{D}[\Omega, \theta(\theta', \phi', \alpha)]| \times A(\theta', \phi') \sin\theta' d\phi' d\theta'. \quad (1)$$

For each signal $S(\Omega, \alpha)$, we solve Eq. (1) using a nonlinear least-squares fit and by parametrization of the molecular frame solution, $|\vec{D}_{\text{Exp}}(\Omega, \theta)|$, using normalized even (0–6, determined by converging fits) Legendre polynomials $[P_{2i}(\theta)]$: $|\vec{D}_{\text{Exp}}(\Omega, \theta)| = |\sum_{i=0}^{3} a_{2i} P_{2i}(\theta)|$. An *a priori* knowledge of the alignment distribution $A(\theta', \phi')$ is required. In our experimental conditions ($P_{\text{back}} = 2$ atm, $T_{\text{rot}} = 30$–40 K, $I_{\text{align}} = 5 \times 10^{13}$ W/cm^2), we estimate achieving a degree of alignment $\langle \cos^2\theta' \rangle = 0.60 \pm 0.05$. Our estimate is supported by recent supersonic gas expansion studies in similar conditions [17]. The corresponding alignment distribution $A(\theta')$ is parametrized analytically [16]. We proceed with a distribution function A that corresponds to $\langle \cos^2\theta' \rangle = 0.60$.

The molecular frame solution to Eq. (1), $\Omega^2 |\vec{D}_{\text{exp}}(\Omega, \theta)|$, is shown in Fig. 2 at both (a) 800 and (b) 1200 nm. We find that, while the lower-order harmonics peak at $\theta = 0°$, higher-order harmonics peak closer to $\theta \sim 35°$ at both laser wavelengths. The retrieved molecular frame profiles depend somewhat on the degree of alignment but the on axis minimum remains similar in the range $0.55 < \langle \cos^2\theta' \rangle < 0.65$. At 1200 nm, the extended cutoff allows us to observe that the spectral minimum is an island near

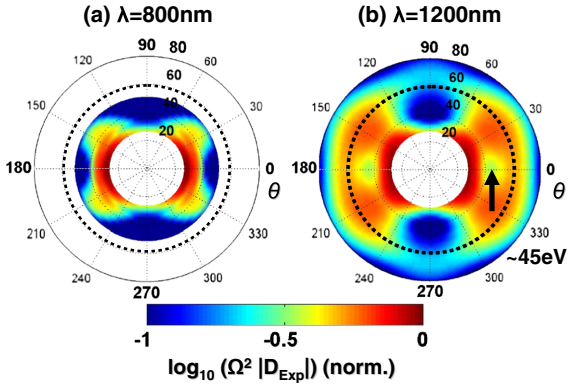

FIG. 2 (color online). Experimental molecular frame transition moments in aligned N_2, derived from the results in Fig. 1. We display the extracted amplitude $\Omega^2 |D_{\text{exp}}(\Omega, \theta)|$ by deconvolving the molecular alignment distribution using Eq. (1). While the laboratory frame signal peaks at $\alpha = 0°$ (see Fig. 1) across the spectrum, in the molecular frame the amplitude instead peaks at a significant angle ($\theta \sim 35°$) between the molecular axis and the laser polarization above 40 eV at 800 nm and at 45 ± 5 eV at 1200 nm.

45 eV and $\theta = 0°$ that is confined in energy and angle. To our knowledge, such features have never before been observed for the HOMO $3\sigma_g$ state of N_2. The $2\sigma_g$ of N_2 photoionization cross sections measured in synchrotron experiments show similar features [8]. Although it is not evident in Fig. 2(a), the island is also present at 800 nm. By normalizing the color scale, the island becomes visible; see Fig. S1 in the supplemental online material [22].

Next, we compare our experimental findings to calculations, both in the molecular and laboratory frames. Photoionization transition moments from the $3\sigma_g$ HOMO orbital of N_2 are calculated in the molecular frame using EPOLYSCAT [23,24]. In Fig. 3(a), the calculated dipole amplitude $\Omega^2|\vec{D}_{\mathrm{calc}}(\Omega,\theta)|$ contains the contributions from both the molecular frame ionization rate (I_{calc}) and recombination amplitude (R_{calc}),

$$|\vec{D}_{\mathrm{calc}}(\Omega,\theta)| = \sqrt{I_{\mathrm{calc}}(\theta)}\sqrt{|\vec{R}_{\mathrm{calc},\parallel}(\Omega,\theta)|^2 + |\vec{R}_{\mathrm{calc},\perp}(\Omega,\theta)|^2}. \tag{2}$$

Equation (2) assumes that the propagation step is not angle dependent. We have used an energy independent recollision amplitude for the electron. This is valid for the plateau harmonics if they are generated with an infrared fundamental beam [13]. At 800 nm, the energy dependence of the recollision amplitude can be removed experimentally using the spectrum of an atomic reference [25].

The molecular frame ionization probability $I_{\mathrm{calc}}(\theta)$, sketched as the solid lines in the middle of the polar plots, is obtained using molecular Ammosov-Delone-Krainov rates [26]. $\vec{R}_{\mathrm{calc}}(\theta)$ is obtained by taking the complex conjugate [27] of the calculated molecular frame photoionization dipoles for the N_2 HOMO only [28]. In good agreement with the experimental result shown in Fig. 2(b), the calculated amplitude in Fig. 3(a) also displays the angular bifurcation starting at ~50 eV and the associated spectral minimum along $\theta = 0°$, centered here at ~58 eV. The strong maximum centered at $\theta = 0°$ and ~35 eV, also partially observed experimentally, is a shape resonance [21].

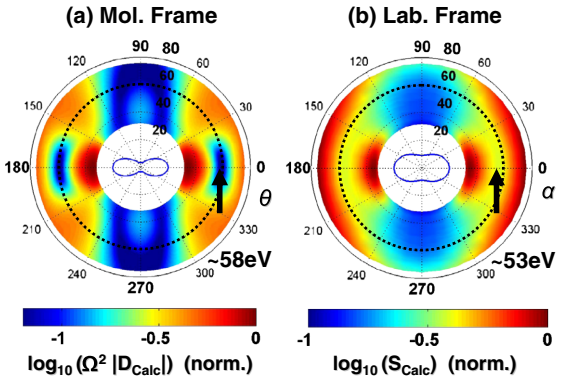

FIG. 3 (color online). Theory: (a) Molecular frame high harmonic amplitude $\Omega^2|D_{\mathrm{calc}}(\Omega,\theta)|$ using calculated differential photoionization dipole matrix elements and analytical angular ionization probabilities. (b) Expected laboratory frame XUV signal $S_{\mathrm{calc}}(\Omega,\theta)$ using Eqs. (1) and (2) to convolve the calculated molecular frame values from (a) with the experimental alignment distribution. The solid line in the middle is the normalized ionization rate in the respective frames calculated using molecular Ammosov-Delone-Krainov rates. The alignment averaging shifts the spectral minimum at $\theta = 0°$ towards lower photon energy and reduces its depth, as seen experimentally.

Although high harmonics are generated primarily from the HOMO due to the exponential sensitivity of tunnel ionization to ionization potential, nevertheless inner valence orbitals can also contribute to the emission [3,5,29]. In N_2, the HOMO-1 is of π_u symmetry, and hence only contributes in the vicinity of 90° [30]. The minimum that is seen in Figs. 2 and 3 is therefore not affected by the HOMO-1. The spectral position of this minimum has been reported to shift to higher photon energy (by ~5 eV, starting from 40 eV) when increasing the driving laser field peak intensity in the range of $I_{\mathrm{probe}} = 1.4\text{–}2.0 \times 10^{14}$ W/cm^2 at 800 nm [20]. Calculations rule out the participation of lower-lying states (HOMO-1 and HOMO-2) to explain this effect [20,30]. Here, working at $I_{\mathrm{probe}} = 1.5 \times 10^{14}$ W/cm^2 insures we are essentially looking at high-harmonic signal coming from HOMO at $\theta = \alpha = 0°$. The HOMO-1 will contribute to the experimental signal around 90° in Fig. 2(b), but not in the calculation in Fig. 3(a), which only considers the HOMO. Elsewhere [21], we are able to reproduce the experimental high-harmonic spectrum at $\alpha = 90°$ by considering the contribution from HOMO-1 [20,29].

In Fig. 3(b), we compute the expected laboratory frame signal $S_{\mathrm{calc}}(\Omega,\alpha)$ using Eqs. (1) and (2). We performed this summation in a coherent fashion (not shown), treating each polarization component separately before summing their square modulus to obtain $S_{\mathrm{calc}}(\Omega,\alpha) = S_{\parallel}(\Omega,\alpha) + S_{\perp}(\Omega,\alpha)$, where

$$S_{\parallel,\perp}(\Omega,\alpha) = \left| \int_{\theta'=0}^{\theta'=\pi} \int_{\phi'=0}^{\phi'=2\pi} \Omega^2 D_{\parallel,\perp}(\Omega,\theta) \times A(\theta',\phi') \sin\theta' d\phi' d\theta' \right|^2, \tag{3}$$

and $D_{\parallel,\perp}(\Omega,\theta) = \sqrt{I_{\mathrm{calc}}(\theta)} \times R_{\parallel,\perp}(\Omega,\theta)$, as similarly defined above in Eq. (2). We observe no significant differences between a coherent and an incoherent sum. In both cases, the Cooper minimum around $\alpha = 0°$ remains quantitatively unchanged, see Fig. S2 in the supplemental information [22]. In the coherent convolution, however, the signal is weaker in the vicinity of $\alpha = 90°$ as a result of destructive interference due to the rapid modulation of the angular phase over the angular width (~25° FWHM) of the alignment distribution; see Eq. (3). We refer the reader to Ref. [28] for the calculated molecular frame dipole phase. Figure 3(b) shows a shallow spectral minimum along $\alpha = 0°$, which now appears at ~53 eV, shifted

to lower photon energy than found (~58 eV) in the molecular frame in Fig. 3(a). The shift depends on the degree of alignment. Experimentally, we observed a similar effect: from ~45 [Fig. 2(b)] to ~42 eV [Fig. 1(b)].

Our calculation also reproduces the measured high-harmonic signal at other angles: at intermediate angles ($\alpha \sim 45°$) the spectral minimum almost disappears then reappears at $\alpha = 90°$. [At all angles, the signal in the cutoff region is stronger than observed experimentally, due to our assumption of a flat recollision amplitude spectrum as a function of energy Ω in Eq. (2)]. Concentrating on $\theta = \alpha = 0°$, our calculations agree well with experiment, the main difference being that the calculated spectral minimum is higher by ~8 eV. Next, we focus on the origin of this spectral minimum.

By symmetry arguments, at $\theta = \alpha = 0°$, only the parallel (to the laser polarization axis) component of the molecular frame recombination dipole $\vec{R}_{\mathrm{calc}}(\theta)$ is nonzero,

$$R_{\mathrm{calc},\parallel}(\theta = 0°) \propto \sum_{i=0}^{\infty} \left\langle \Psi_g^N | r | \hat{A} \Psi_g^{N-1} \Psi_{c,l=2i+1} \right\rangle, \qquad (4)$$

where Ψ_g^N is the HOMO of N_2 from a Hartree-Fock calculation using a correlation-consistent valence-triple-zeta (cc-pVTZ) basis set using GAMESS [31], Ψ_g^{N-1} is the correlated $N-1$ electron ion core wave function, $\Psi_{c,l}$ are the one-electron continuum scattering states with Σ_u symmetry, and $\hat{A}$ is the appropriate antisymmetrization operator [11]. Equation (4) is expanded in terms of spherical harmonics $Y_l^{m=0}$ and the corresponding radial parts are solved numerically by EPOLYSCAT [23,24].

In Fig. 4, we decompose $R_{\mathrm{calc},\parallel}(\theta = 0°)$ into its partial waves (l) contributions. The two dominant components, the $l = 1$ and 3 partial waves (p and f waves), are out of phase at ~58 eV, see Fig. 4(b), while their amplitudes are similar, see Fig. 4(a). The interference gives rise to a strong spectral minimum in the molecular amplitude, shown as the solid line in Fig. 4(c), and a less deep minimum in the expected laboratory frame spectral intensity; see dashed line in Fig. 4(c). This electronic structural minimum is analogous to the Cooper minimum [32] seen in argon [27]. In molecular photoionization, this type of interference is also referred to as a Cohen-Fano interference [33,34]. In the molecular frame, this spectral feature correlates to a $\sim\pi$ radian phase jump, while in the laboratory frame, after coherent averaging along the lines of Eqs. (1) and (2), it is only about $\pi/3$ radians; see Fig. 4(d). This is in good agreement with recent phase measurements which observe a smaller than π phase jump around the spectral minimum at $\alpha = 0°$ [3,35].

Recent transient grating measurements allowed the angular amplitude and phase of aligned N_2 molecules to be retrieved [28]. They show the shape resonance around (~35 eV), however, due to the use of an 800 nm laser source, the Cooper minimum could not be resolved. To summarize, in aligned N_2 ($\theta = \alpha = 0°$), our calculations predict the co-existence of adjacent but spectrally separated features in the molecular frame: (i) the shape resonance [21] represented by the local amplitude maximum at low photon energy (~35 eV) followed by (ii) a local phase maximum (~50 eV), then (iii) the Cooper-like minimum at higher energy (~58 eV) accompanied with a rapid π phase change.

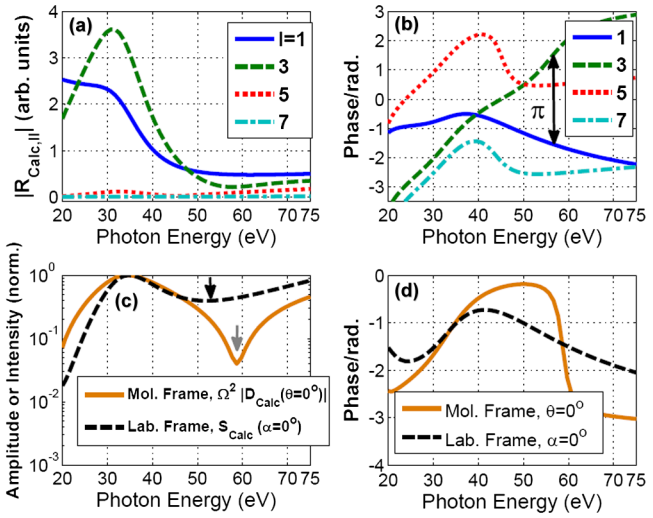

FIG. 4 (color online). Decomposing the calculated photorecombination dipole $R_{\mathrm{calc},\parallel}(\theta = 0°)$ into contributions from the different partial spherical waves (l) describing the continuum Σ_u state in aligned ($\theta = 0°$) N_2: (a) their relative amplitudes and (b) phases. A π phase difference between the dominant $l = 1$ and 3 (p and f waves) components explains the strong spectral minimum at ~58 eV. This molecular electronic structural minimum is analogous to the Cooper minimum probed in argon [27] by high harmonic generation. (c–d) The calculated amplitude (c) and phase (d) in the molecular frame (solid line) and in the laboratory frame (dashed line).

Our results show that we are able to extract molecular frame recombination transition moments from high harmonic measurements of aligned N_2 molecules. By deconvolving the axis alignment distribution, we are able to identify a minimum in the transition moment at 45 eV. Molecular frame photoionization calculations show qualitative agreement with the experiment, exhibiting a deep minimum at 58 eV. We provide an interpretation for this structural Cooper-like minimum, which can be disentangled from a dynamical minimum underlying multielectron hole dynamics [3,5,36]: the latter minimum shifts spectrally both with driving laser intensity and wavelength [5,18]. The good agreement between experiment and theory further evidences that high-harmonic spectroscopy is a measure of field-free photorecombination dipole matrix elements [11,12,27]. The procedure that we have introduced will be particularly important for dynamic imaging of photoinduced chemical reactions [6,7,37] for which little *a priori* knowledge of the high-harmonic dipole is available. For example, it will be helpful for photoexcitation where we know the angular distribution of excited molecules exactly.

Our results are also important for the tomographic reconstruction of molecular orbitals [2]. In Ref. [2], the authors assumed a π phase jump in the transition moment at 40 eV, on the basis of the observed minimum in the harmonic spectrum. In the present Letter, we show that the deconvolution procedure moves this minimum to 45 eV. The EPOLYSCAT results confirm that it is indeed a π phase jump in the molecular frame. Incorporating the more accurate measurements into the tomographic procedure would reduce the observed internuclear spacing by 5%, demonstrating the accuracy of the technique.

Looking forward, it is experimentally feasible to simultaneously measure the ionization probability and the harmonic spectrum as a function of alignment angle [38,39]. This dual procedure would further refine high-harmonic molecular frame photorecombination measurements by removing the contribution from the ionization step. We believe that high-harmonic spectroscopy will provide unparalleled resolution of the molecular frame photoionization or recombination cross section of high-lying orbitals for many molecules that can be laser aligned.

We thank P. Salières for fruitful discussions. We acknowledge funding from NSERC, CIPI, and AFOSR.

[1] A.-T. Le, R. R. Lucchese, M. T. Lee, and C. D. Lin, Phys. Rev. Lett. **102**, 203001 (2009).
[2] J. Itatani, J. Levesque, D. Zeidler, H. Niikura, H. Pépin, J. C. Kieffer, P. B. Corkum, and D. M. Villeneuve, Nature (London) **432**, 867 (2004).
[3] S. Haessler, J. Caillat, W. Boutu, C. Giovanetti-Teixeira, T. Ruchon, T. Auguste, Z. Diveki, P. Breger, A. Maquet, and B. Carré *et al.*, Nature Phys. **6**, 200 (2010).
[4] C. Vozzi, M. Negro, F. Calegari, G. Sansone, M. Nisoli, S. D. Silvestri, and S. Stagira, Nature Phys. **7**, 822 (2011).
[5] O. Smirnova, Y. Mairesse, S. Patchkovskii, N. Dudovich, D. M. Villeneuve, P. B. Corkum, and M. Y. Ivanov, Nature (London) **460**, 972 (2009).
[6] H. J. Wörner, J. B. Bertrand, D. V. Kartashov, P. B. Corkum, and D. M. Villeneuve, Nature (London) **466**, 604 (2010).
[7] H. J. Wörner, J. B. Bertrand, B. Fabre, J. Higuet, H. Ruf, A. Dubrouil, S. Patchkovskii, M. Spanner, Y. Mairesse, and V. Blanchet *et al.*, Science **334**, 208 (2011).
[8] S. Motoki, J. Adachi, K. Ito, K. Ishii, K. Soejima, A. Yagishita, S. K. Semenov, and N. A. Cherepkov, Phys. Rev. Lett. **88**, 063003 (2002).
[9] W. Guo, B. Yang, C.-x. Wang, K. Harkay, and M. Borland, Phys. Rev. ST Accel. Beams **10**, 020701 (2007).
[10] H. Stapelfeldt and T. Seideman, Rev. Mod. Phys. **75**, 543 (2003).
[11] A.-T. Le, R. R. Lucchese, S. Tonzani, T. Morishita, and C. D. Lin, Phys. Rev. A **80**, 013401 (2009).
[12] M. V. Frolov, N. L. Manakov, T. S. Sarantseva, and A. F. Starace, Phys. Rev. A **83**, 043416 (2011).
[13] A. D. Shiner, B. E. Schmidt, C. Trallero-Herrero, H. J. Wörner, S. Patchkovskii, P. B. Corkum, J.-C. Kieffer, F. Légaré, and D. M. Villeneuve, Nature Phys. **7**, 464 (2011).
[14] P. B. Corkum and F. Krausz, Nature Phys. **3**, 381 (2007).
[15] A. Scrinzi, M. Y. Ivanov, R. Kienberger, and D. M. Villeneuve, J. Phys. B **39**, R1 (2006).
[16] D. Pavičić, K. F. Lee, D. M. Rayner, P. B. Corkum, and D. M. Villeneuve, Phys. Rev. Lett. **98**, 243001 (2007).
[17] K. Yoshii, G. Miyaji, and K. Miyazaki, Phys. Rev. Lett. **106**, 013904 (2011).
[18] H. J. Wörner, J. B. Bertrand, P. Hockett, P. B. Corkum, and D. M. Villeneuve, Phys. Rev. Lett. **104**, 233904 (2010).
[19] R. Torres, T. Siegel, L. Brugnera, I. Procino, J. G. Underwood, C. Altucci, R. Velotta, E. Springate, C. Froud, and I. C. E. Turcu *et al.*, Opt. Express **18**, 3174 (2010).
[20] J. Farrell, B. McFarland, M. Gühr, and P. Bucksbaum, Chem. Phys. **366**, 15 (2009).
[21] C. Jin, J. B. Bertrand, R. R. Lucchese, H. J. Wörner, P. B. Corkum, D. M. Villeneuve, A.-T. Le, and C. D. Lin, Phys. Rev. A **85**, 013405 (2012).
[22] See Supplemental Material at http://link.aps.org/supplemental/10.1103/PhysRevLett.109.143001 for visualizing Fig. 2(a) using another normalization and Fig. 3(b) obtained using different levels of approximation in Eq. (1).
[23] F. A. Gianturco, R. R. Lucchese, and N. Sanna, J. Chem. Phys. **100**, 6464 (1994).
[24] A. P. P. Natalense and R. R. Lucchese, J. Chem. Phys. **111**, 5344 (1999).
[25] J. Levesque, D. Zeidler, J. P. Marangos, P. B. Corkum, and D. M. Villeneuve, Phys. Rev. Lett. **98**, 183903 (2007).
[26] X. M. Tong, Z. X. Zhao, and C. D. Lin, Phys. Rev. A **66**, 033402 (2002).
[27] H. J. Wörner, H. Niikura, J. B. Bertrand, P. B. Corkum, and D. M. Villeneuve, Phys. Rev. Lett. **102**, 103901 (2009).
[28] A. Rupenyan, J. B. Bertrand, D. M. Villeneuve, and H. J. Wörner, Phys. Rev. Lett. **108**, 033903 (2012).
[29] B. K. McFarland, J. P. Farrell, P. H. Bucksbaum, and M. Gühr, Science **322**, 1232 (2008).
[30] A.-T. Le, R. R. Lucchese, and C. D. Lin, J. Phys. B **42**, 211001 (2009).
[31] M. W. Schmidt, K. K. Baldridge, J. A. Boatz, S. T. Elbert, M. S. Gordon, J. H. Jensen, S. Koseki, N. Matsunaga, K. A. Nguyen, and S. Su *et al.*, J. Comput. Chem. **14**, 1347 (1993).
[32] J. W. Cooper, Phys. Rev. **128**, 681 (1962).
[33] H. D. Cohen and U. Fano, Phys. Rev. **150**, 30 (1966).
[34] R. Della Picca, P. D. Fainstein, M. L. Martiarena, N. Sisourat, and A. Dubois, Phys. Rev. A **79**, 032702 (2009).
[35] B. K. McFarland, J. P. Farrell, P. H. Bucksbaum, and M. Gühr, Phys. Rev. A **80**, 033412 (2009).
[36] E. Goulielmakis, Z.-H. Loh, A. Wirth, R. Santra, N. Rohringer, V. S. Yakovlev, S. Zherebtsov, T. Pfeifer, A. M. Azzeer, M. F. Kling *et al.*, Nature (London) **466**, 739 (2010).
[37] H. J. Wörner, J. B. Bertrand, P. B. Corkum, and D. M. Villeneuve, Phys. Rev. Lett. **105**, 103002 (2010).
[38] T. Kanai, S. Minemoto, and H. Sakai, Nature (London) **435**, 470 (2005).
[39] H. Akagi, L. Arissian, J. B. Bertrand, P. B. Corkum, M. Gertsvolf, D. Pavičić, D. M. Rayner, C. Smeenk, A. Staudte, and D. M. Villeneuve *et al.*, Laser Phys. **19**, 1697 (2009).